Theoretical Study on the Properties of Linear and Cyclic Amides in Gas Phase and Water Solution

S. Aparicio-Martínez,*,† K. R. Hall, and P. B. Balbuena*

Artie McFerrin Department of Chemical Engineering, Texas A&M University, College Station, Texas 77843

Received: February 21, 2006; In Final Form: April 30, 2006

The structural and energetic properties of a group of selected amides, of well-known importance for the design of efficient clathrate inhibitors, are calculated with Hartree−Fock and density functional theory, B3LYP, theoretical levels, and a 6-311++g** basis set in the gas phase and a water solution. The conformational behavior of the molecules is studied through the scanning of the torsional potential energy surfaces and by the analysis of the differences in the energetic and structural properties between the isomers. The properties of the amides in water solution are determined within a self-consistent reaction field approach with a polarizable continuum model that allows the calculation of the different contributions to the free energy of solvation. The calculated barriers to rotation are in good agreement with the available experimental data and the comparison of the gas and water results shows the strong effect of the solute polarization. The properties of different amide−water complexes are calculated and compared with available experimental information.

Introduction

The study of the properties of linear and cyclic amides in the gas phase and a water solution is very important from theoretical and practical viewpoints. Amides have been extensively studied both theoretically and experimentally from a number of perspectives. For biological purposes, amides may be considered as models of peptidic bonds[1−3] because of their presence as repeating units in biological macromolecules. The understanding of the properties of these complex biomolecules requires the accurate knowledge of nonbonded interactions, such as the intramolecular amide−amide and the intermolecular amide−water hydrogen bondings,[4,5] which are key contributors to the specificity of the interactions within and between macromolecules and that can be modeled through the study of the simpler amide molecules.[6−8]

Among the most promising applications of amides are those related with their use as very effective kinetics inhibitors of the crystallization of gas hydrates. The hydrate formation is a major problem for the gas industry because conditions found during natural gas exploration, processing, and transportation are frequently optimal for hydrate formation in pipelines and processing equipment.[9,10] Most current methods to avoid hydrate formation are based in the shifting of the boundaries of phase diagrams toward more extreme conditions of pressure and temperature, mainly through injection of large amounts of methanol, but this thermodynamic method is economically very costly and environmentally hazardous.[11] A more promising approach has been developed in the last years with the discovery of the so-called low dosage inhibitors (LDI) that work in very low concentrations and whose effect is produced by a kinetic mechanism in which the onset of the hydrate formation is delayed. Many of the more efficient kinetic inhibitors are monomers or polymers of the amide type such as acrylamide, *N*-vinyl-2-pyrrolidone, or poly(*N*-vinyl-2-pyrrolidone).[12,13] Previous theoretical studies of these compounds in water solution have shown that LDI acts by reducing the structureness of the surrounding water solvent and, thus, probably increasing the barrier to hydrate nucleation.[14−16] Thus, the knowledge of the microscopic behavior and properties of amides in water solution obtained through theoretical studies may help to develop more efficient hydrate inhibitors because the inherent experimental complexity related with these kind of systems makes it difficult to compare directly the effects of inhibitors on the macroscopic kinetics of hydrate formation.

The aim of this work is to gain a deeper insight through quantum computations into the structural and energetic properties of amides in gas phase and in very diluted aqueous solutions, where only solute−solvent interactions are relevant. The information obtained may serve to understand the electronic origin of the factors that determine the properties of these simple molecules, and to get insights into the more complex ones in which the amide bond is involved, such as proteins or clathrate inhibitor polymers, and how they are affected by the water environment. Also, it may be useful to study the water−amide interaction at a molecular level, which is extremely important to confirm the structuring effect that these molecules may have on the surrounding water medium.

The conformational behavior of amides, peptides, and proteins is constrained by the geometrical properties of the amide bond, such as the almost planarity around the C−N bond that shows a partial double-bond character. The well-known trans preference of *N*-monosubstitute amides and proteins is not well understood yet, although it is supposed to be originated by a complex combination of steric and charge interaction factors,[17] but the effect of the solvent on the torsional barriers and on the cis/trans ratios is not yet clear. The determination of the properties of isomers through high-level quantum computations and the detailed analysis of the torsional potential energy profiles may provide information to understand the nature of the preferred isomers and how this phenomenon is affected by the water medium.

* To whom correspondence should be addressed. E-mail: sapar@ubu.es (S.A.-M.); balbuena@tamu.edu (P.B.B.).

† Permanent address: Department of Chemistry, University of Burgos, 09001 Burgos, Spain.

10.1021/jp0611166 CCC: $33.50
Published on Web 06/29/2006

Eight amides were selected in this work with the criterion of their validity for the study of the amide bond properties and for identifying the preferred isomers, and also because of their importance in the clathrate inhibitor process. The studied compounds are: *N*-methylformamide (NMF), *N*-ethylformamide (NEF), *N*-methylacetamide (NMA), *N*-ethylacetamide (NEA), acrylamide (ACA), *N*-vinylformamide (VYF), *N*-vinyl-2-pyrrolidone (VYP), and *N*-vinyl-2-piperidone (VYPP). We report quantum calculations at Hartree−Fock (HF) and density functional theory (DFT) levels of the molecular properties in the gas phase and water solutions. The energy differences, torsional energy profiles, and ratios between the different isomers for each compound are also calculated, and the water effect on these properties is analyzed. Finally, the properties of several amide/water complexes are calculated to establish how the structure of the amide affects the specific interactions through hydrogen bonding with water and how this effect can be related with the proposed structuring effect of amides on the water-surrounding medium.

Methods

The HF and DFT computations were done with the Gaussian 98 package.[18] The DFT studies employed the Becke gradient corrected exchange functional[19] in conjunction with the Lee−Yang−Parr correlation functional[20] with the three parameters (B3LYP)[21] method. B3LYP is a gradient corrected method that includes some of the effects of electron correlations. This DFT approach usually gives rise to greater accuracy than HF for structure, thermochemistry, and spectroscopic properties,[22] with only a slightly greater computational effort; this combination of efficiency and accuracy has made it perhaps the most popular method for practical applications. Results obtained with both HF and DFT approaches are compared with experimental ones when available.

The computations reported in this work may be divided into three groups:

(i) Gas-phase calculations are done with the 6-311++g** basis set at HF and B3LYP levels to determine the geometric and energetic parameters of the different isomers and to establish the most stable ones. We have also calculated the torsional barriers through relaxed scanning of the torsional potential energy surfaces (PES) at 10° intervals with a 6-31+g* basis set at both theoretical levels; in this scanning procedure for each change of the corresponding torsional angle, the structure is fully optimized for that fixed value of the angle relaxing the other degrees of freedom.

(ii) Water solution calculations, done within the self-consistent reaction field approach (SCRF) in which the solvent is treated as a continuum. We adopted the polarizable continuum model (PCM)[23] because it provides a quantitative estimation of the different contributions to the total free energy of solvation. Although the SCRF methods do not account for specific solute−solvent interactions, such as hydrogen bonding, and results based on these methods are clearly dependent on the selected size and shape of the solute cavity, they proved to be successful on analysis of the effect of solvents on solute properties and on isomer ratios.[17,25] The coupling of PCM models with DFT to study the interactions of solutes and solvents is not as frequent as with HF; in this work the properties of the amides in solution were calculated at both theoretical levels with a 6-311++g** basis set, except for the PES that was calculated using the 6-31+g* basis set. All the SCRF calculations were done through fully optimization of the structures with the gas-phase geometries as initial guesses. The molecule−shaped cavity is constructed as the union of interlocking spheres where the scaling factor for radius is 1.2 and 60 triangular tesserae per sphere are considered. Comparison of gas and solution results allows clarifying the solute polarization effect.

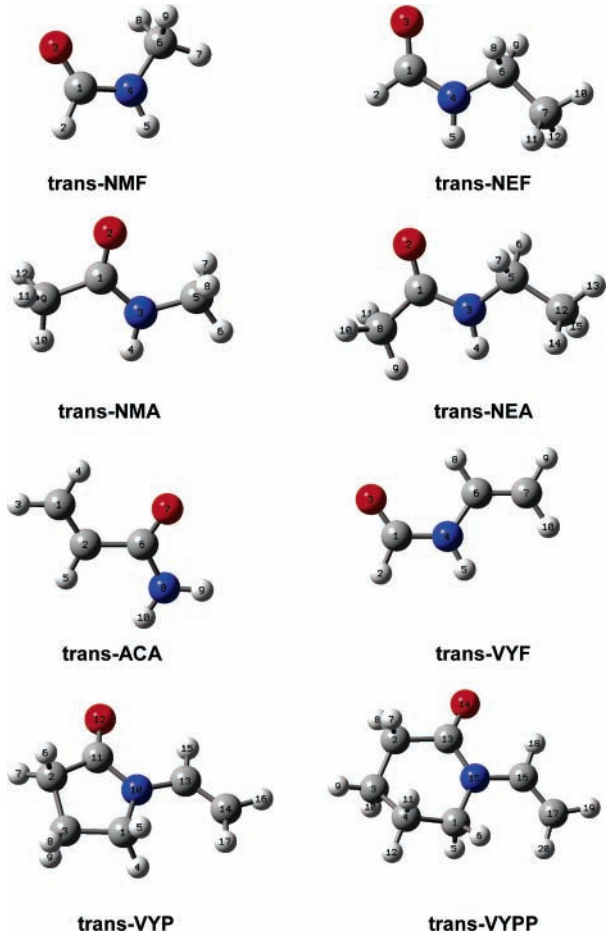

Figure 1. Optimized structures of the lowest energy isomers in the gas phase calculated with the HF/6-311++G** method.

(iii) The properties of several amide/water complexes were computed and their structures optimized at B3LYP levels with the 6-31+g* basis set.

Results and Discussion

Gas Phase. The structures of the lowest energy isomers for each compound are reported in Figure 1, and molecular parameters (geometries, charges) are in Table 1 (Supporting Information). For *N*-substituted linear amides (NMF, NEF, NMA, NEA, and VYF), trans means that the oxygen atom and the hydrogen connected to nitrogen are at opposite sides of the C−N bond, and thus, going from cis to trans implies torsions around the C(O)−N bond. For ACA, trans means that the oxygen and the hydrogen attached to the first carbon of the vinyl group (numbered as 5 in Figure 1) are at opposite sides of the C−C bond, and thus, going from cis to trans implies turning around the C(O)−C bond. Finally, for the cyclic amides VYP and VYPP, trans refers that the C(O) and the final carbon of the vinyl group are at opposite sides of the molecule, and thus, going from cis to trans implies torsions around the N−C(vinyl) bond.

The calculated energy differences between the isomers are reported in Table 1, and the dipole moments are in Table 2. For *N*-substituted linear amides, the trans isomers are always the lowest-energy ones, as is reported in literature.[17,28,29] The

TABLE 1: Calculated Energy Differences between the Cis and Trans Isomers, $\Delta E = (E_{cis} - E_{trans})$/kcal mol^{-1}, in the Gas Phase and in Water Solution with the PCM Model and the Reported Theoretical Levels

	NMF	NEF	NMA	NEA	ACA	VYF	VYP	VYPP
				gas phase				
HF/6-311++g**	1.14	1.01	2.53	2.42	1.47	0.51	3.47	4.40
B3LYP/6-311++g**	0.92	0.89	2.28	2.48	1.38	0.18	3.26	2.92
				water solution				
HF/6-311++g**	0.58	−0.43	2.75	2.24	1.58	0.10	2.88	3.20
B3LYP/6-311++g**	0.03	0.24	2.45	2.08	1.53	−0.11	2.68	2.83

TABLE 2: Calculated Dipole Moments for the Cis and Trans Isomers, μ/Debye, in the Gas Phase

	NMF	NEF	NMA	NEA	ACA	VYF	VYP	VYPP
				gas phase				
HF/6-311++g** cis	4.53	5.14	4.41	4.54	4.20	3.34	5.06	4.65
B3LYP/6-311++g** cis	4.40	4.93	4.29	4.44	4.01	3.20	4.72	4.84
HF/6-311++g** trans	4.30	4.73	4.17	4.15	3.87	3.73	4.66	4.33
B3LYP/6-311++g** trans	4.12	4.36	4.02	3.87	3.76	3.63	4.36	4.30
Experimental trans	3.78[a]		3.87[b]					
				water solution				
HF/6-311++g** cis	6.06	6.20	5.96	6.19	5.79	4.38	6.93	6.81
B3LYP/6-311++g** cis	6.07	6.21	5.99	6.21	5.67	4.31	6.84	
HF/6-311++g** trans	5.93	5.87	5.95	5.81	5.48	5.05	6.11	6.01
B3LYP/6-311++g** trans	5.94	5.98	5.93	5.84	5.55	5.03	6.05	5.94

[a] Ref 26. [b] Ref 27 (in CCl_4).

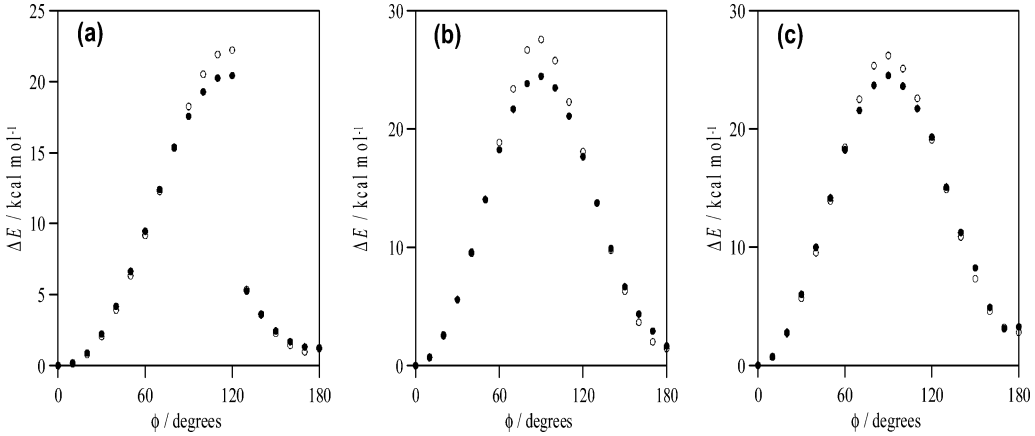

Figure 2. Calculated relaxed potential energy scanning for the dihedral angle O−C(O)−N−C (3−1−4−6 in Figure 1) in NMF using (a) redundant and (b) nonredundant torsion coordinates. ϕ, dihedral angle; ΔE, energy relatives to the minimum value ($\phi = 0$). (c) Calculated relaxed potential energy scanning for the dihedral angle O−C(O)−N−C (2−1−3−5 in Figure 1) in NMA using nonredundant torsion coordinates. ϕ, dihedral angle; ΔE, energy relatives to the minimum value ($\phi = 0$). (●) HF/6-31+g*, (○) B3LYP/6-31+g*.

ability of the nitrogen in the amide bond to delocalize its electron lone pair imposes a character of partial double bond to the C(O)−N bond and, thus, a planarity to the amide bond moiety. Hence, this planar character determines the torsional profile for going from cis to trans conformers in linear amides. A rotation around the C(O)−N amide bond will go through a energy maximum at 90° with energy minima only at 0° (cis) and 180° (trans) dihedrals; these minima appear as a consequence of the resonance stabilization obtained at these angles, which is almost half of the total rotational barrier.[30] The calculation of torsional barriers by scanning the potential energy surface presents some problems related with the use of redundant coordinates, mainly because if redundant torsion and out-of-plane bending coordinates are mistakenly used for unsaturated bonds such as C(O)−N, then the torsional barriers are not calculated correctly.[31] This is clearly shown in Figure 2, where the NMF torsional barrier is calculated with redundant and nonredundant coordinates. The use of redundant coordinates gives rise to unphysical results both with HF and B3LYP, Figure 2a, with a sudden jump in the relative energy at around 120°. However, the use of nonredundant coordinates produces the correct profile, Figure 2b, with a transition state at 90° with $\Delta E = 27.6$ kcal mol^{-1}.

The trans preference has been frequently justified considering steric factors: the strain produced by the *N*-substitute in a cis conformer;[32] nevertheless, this does not justify such preference in formamides for which the steric effect should not be the main one. In this case, the electrostatic interaction may play a main role.[17] To confirm this hypothesis, the highly occupied molecular orbitals (HOMO) and electronic density surfaces are plotted for NMF in Figure 3. In the trans conformer, the close proximity of the hydrogen in *N*-methyl group (Figure 3), which is electron deficient, to the negatively charged oxygen causes a negative electrostatic contribution (~ -9.5 kcal mol^{-1}, calculated considering a Coulombic potential and charges and distances from HF/6-311++g**, Table 1 Supporting Information), to the total potential. Figure 3 shows the clear difference between both isomers; for the trans isomer, the methyl hydrogen and the oxygen interact electrostatically, as is illustrated by he HOMO shape in contrast with the shape of the cis isomer at the same isovalue. The calculated dipole moments are reported in Table 2 for both isomers; for *N*-alkylamides, the dipole moments of the trans isomers are always lower than those for the cis ones. The moments for *N*-alkylamides are almost parallel to the C(O)−O bond, see Table 1 (Supporting Information).

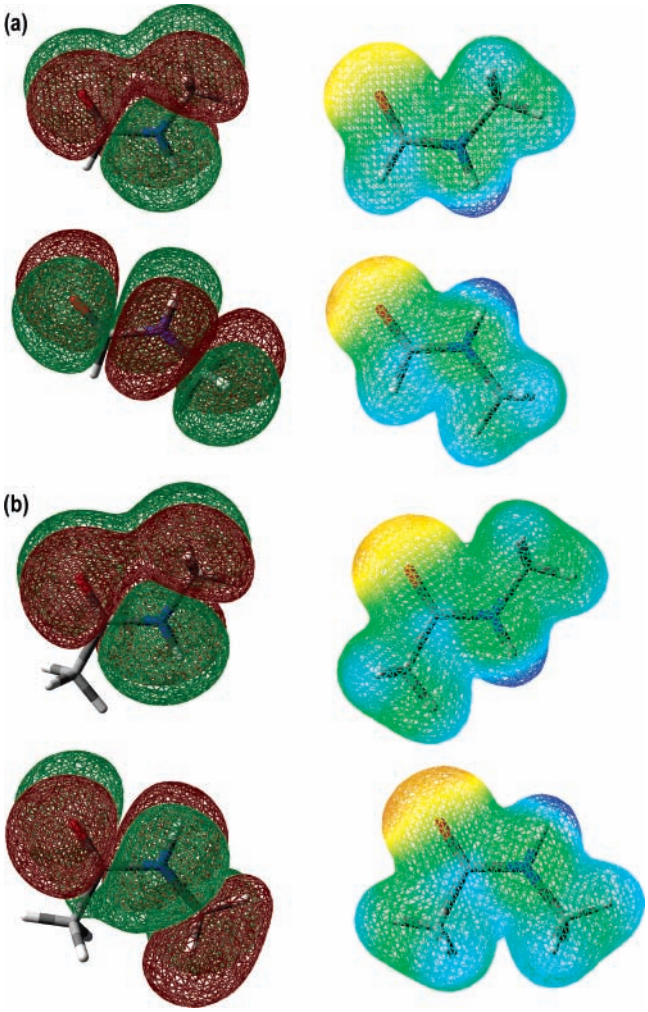

Figure 3. (a) Calculated, HF/6-311++g**, HOMO (left) and electron density (right) surfaces for trans and cis conformers of NMF. Isosurface value = 0.01 e/Å^3. (b) Calculated, HF/6-311++g**, HOMO (left) and electron density (right) surfaces for trans and cis conformers of NMA. Isosurface value = 0.01 e/Å^3.

The effect of the presence of substituents on the carbonyl side of the amide moiety is analyzed with NMA and NEA. The energy difference between cis and trans isomers is slightly greater for NMA than for NMF, Table 1, but the energy of the transition state, $\phi = 90°$, estimated from the potential scan, Figure 2c, is almost the same for both molecules (for NMA, $\Delta E = 26.2$ kcal mol^{-1} at $\phi = 90°$, only 1.4 kcal mol^{-1} smaller than for NMF). The presence of the methyl group, which acts as an electron-releasing group, attached to the carbonyl should affect the properties of the cis/trans transition, but although the methyl group increases the energy of the cis conformer, the rotational barrier is almost the same for both compounds, as seen in Figure 2. The presence of the electron-donating substituent in the carbonyl side of the molecules should decrease the torsional barrier,[35] but such an effect is not very important in the case of the methyl group in NMA. Figure 3b illustrates that the calculated HOMO and electron density surfaces for NMA are very close to those for NMF (Figure 3a), suggesting that the main effect for the trans stabilization is the electrostatic interaction between the oxygen and the hydrogen in the methyl group of the nitrogen side. The increase in the energetic difference between both isomers could be produced by an additional steric contribution because of the close interaction between both methyl groups in the cis conformation of NMA; this is confirmed by the increase of the C(O)−N bond length that is 0.007 Å longer for the cis isomer according to HF/6-311++g** and 0.0053 Å according to B3LYP/6-311++g** results. For NMF, the C(O)−N has almost the same length for both conformations with HF and B3LYP calculations.

The energy differences between the isomers decrease slightly with the increasing size of the *N*-substituent (Table 1), as observed from NMR studies.[30] The calculated torsional barriers for NEF and NEA are reported in Figure 4; these barriers are almost identical to those for NMF and NMA, respectively (NEF: $\Delta E = 27.4$ kcal mol^{-1}, NEA: $\Delta E = 25.6$ kcal mol^{-1}, both at $\phi = 90°$). To illustrate this point, we have also included in Figure 4 the results of the calculations of the torsional barrier for the *N*-*tert*-butylformamide (NTBF), which contains a voluminous group in the nitrogen side of the peptide bond. The results for NTBF confirms the small effect of the *N*-substituent on the torsional barrier for this voluminous substituent, $\Delta E = 27.0$ kcal mol^{-1} at $\phi = 90°$, i.e., only 0.6 kcal mol^{-1} smaller than that for NMF. Thus, the introduction of more voluminous groups in the nitrogen side of the amide bond does not affect substantially the energy of the transition state; it only decreases slightly the energy difference between the cis and trans conformers, but it seems clear from the results that the main effect for the stabilization of trans isomer is the interaction with the oxygen atom; this also affects the torsional barrier because this interaction is weakened or lost for values of the torsional angle different from zero (trans configuration), as is shown in Figure 4 for NEF. This seems to be characteristic of the peptide bond. On the other side, the C(O)−N is almost constant for the studied amides (∼1.36 Å, at B3LYP/6-311++g** level, Table 1, Supporting Information), and thus, the torsional barrier is only slightly affected by the size of the *N*-substituent.

The presence of more complex substituents in the nitrogen side of the amide bond is analyzed with VYF. There are four possible conformers for this molecule, Figure 5; from the calculated values of energy it is clear that isomers 1 and 2 (trans and cis, respectively) are the ones with the lowest energies; data for these isomers are reported in Tables 1 and 2, and torsional barriers are reported in Figure 5. The energy difference between cis and trans isomers in VYF is almost negligible, Table 1, and the dipole moments of both conformers are almost the same. Although in the available literature it is claimed that the cis conformer should predominate,[35] Table 1 illustrates that the trans conformer has the lowest energy. The HOMO features of both isomers (Figure 5) show how the interaction between the hydrogen of the vinyl group and the oxygen is less effective than in the aforementioned amides, because of the planar character imposed by the vinyl group double bond. The bond C(O)−N is longer for VYF than for the other *N*-substituted studied amides (Table 1, Supporting Information); thus, the bond order decreases, and accordingly, the torsional barrier ($\Delta E = 24.1$ kcal mol^{-1} at $\phi = 90°$ with B3LYP/6-311++g**) is smaller than those for other amides such as NEF.

The effect of the presence of the vinyl group in the carbonyl side of the amide bond is studied with ACA. Table 1 shows two possible conformers for this molecule; the most stable is the trans isomer in which the vinyl double bond and the carbonyl group are in the same side (trans, Figure 1), in accordance with IR-vapor phase and microwave data reported in the literature.[36,37] The calculated rotational barrier, Figure 6, for the trans−cis transition in ACA is much smaller than those obtained for the previous amides because the rotation for ACA implies a C−C(O) rotation instead of C(O)−N. The reported values of the activation energy for the trans−cis conversion are concordant with those reported at various theoretical levels.[38,39] The

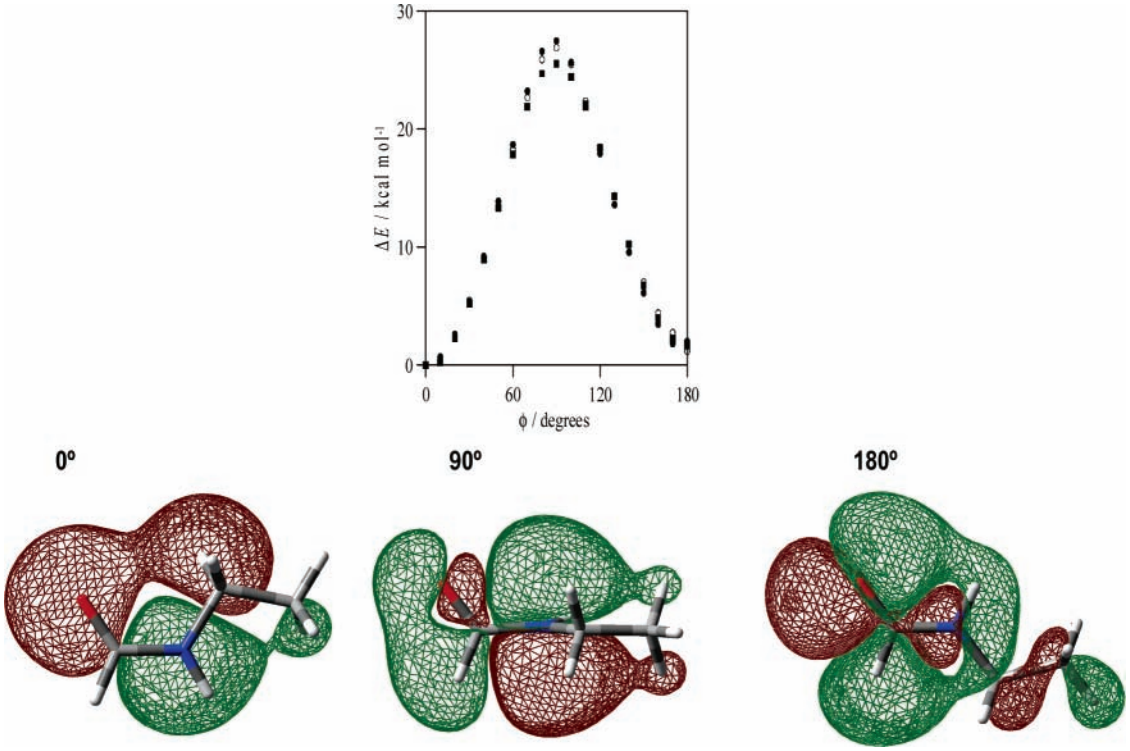

Figure 4. (Top) Calculated relaxed potential energy scanning for the dihedral angle O−C(O)−N−C (3−1−4−6 in Figure 1) in NEF, NTBF, and NEA (2−1−3−5 in Figure 1) using nonredundant torsion coordinates and B3LYP/6-31+g* theoretical level. ϕ, dihedral angle; ΔE, energy relatives to the minimum value ($\phi = 0$). (●) Nef, (○) Ntbf, and (■) NEA. (Bottom) Calculated, HF/6-311++g**, HOMO surfaces for different values of the dihedral angle O−C(O)−N−C (2−1−3−5 in Figure 1) in NEF. Isosurface value = 0.01 e/Å^3.

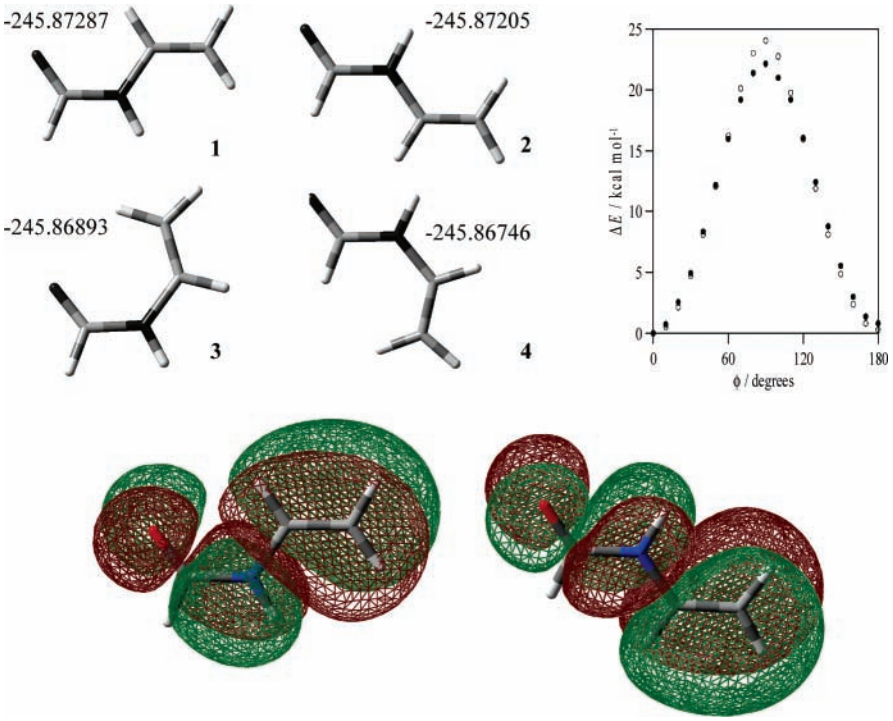

Figure 5. (Top, left) Conformers for VYF with energies (Hartree) calculated at HF/6-311++g** level. (Top, right) Calculated relaxed potential energy scanning for the dihedral angle O−C(O)−N−C (3−1−4−6 in Figure 1) in VYF using nonredundant torsion coordinates. ϕ, dihedral angle; ΔE, energy relatives to the minimum value ($\phi = 0$). (●) HF/6-31+g*, (○) B3LYP/6-31+g*. (Bottom) Calculated, HF/6-311++g**, HOMO surfaces for trans and cis conformers of VYF. Isosurface value = 0.01 e/Å^3.

structure of *trans*-ACA is planar, as is shown by the components of the dipole moment reported in Table 1 (Supporting Information), whereas the cis isomer is slightly skewed (see the minima around $\phi = 160°$ in Figure 6). The HF/6-311++g** HOMO calculated for both isomers of ACA are reported in Figure 7; the shape of these orbitals is almost the same for the cis and trans isomers and very different to those reported for VYF, Figure 5. For VYF, the rotation around the C(O)−N bond produces an inversion of the HOMO phases in the carbonyl and nitrogen group (Figure 5). Thus, the phase pattern of the HOMO in VYF, and hence the electron distribution in the linear combination, is determined by the position of the *N*-vinyl group.

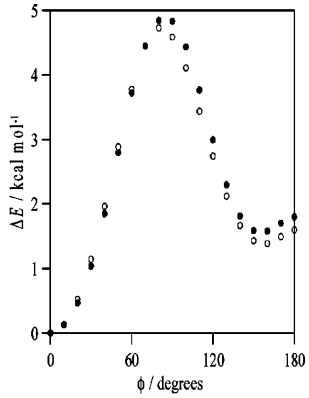

Figure 6. Calculated relaxed potential energy scanning for the dihedral angle O−C(O)−C−C (7−6−2−1 in Figure 1) in ACA. ϕ, dihedral angle; ΔE, energy relatives to the minimum value ($\phi = 0$). (●) HF/6-31+g*, (○) B3LYP/6-31+g*.

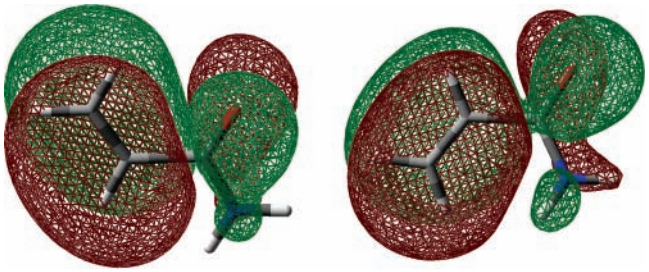

Figure 7. Calculated, HF/6-311++g**, HOMO surfaces for trans and cis conformers of ACA. Isosurface value = 0.01 e/Å^3.

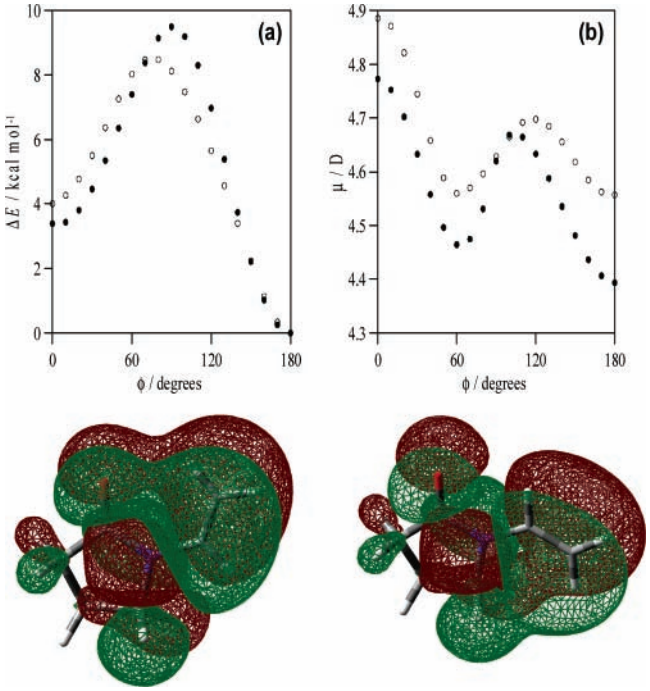

Figure 8. (Top) Calculated relaxed potential energy scanning for the dihedral angle C(O)−N−C−C (11−10−13−14 and 13−15−16−17 in Figure 1) in VYP and VYPP at B3LYP/6-31+g* theoretical level. ϕ, dihedral angle; ΔE, energy relatives to the minimum value (ϕ = 180) and μ, dipole moment. (●) VYP, (○) VYPP. (Bottom) Calculated, HF/6-311++g**, HOMO surfaces for trans and cis conformers of VYP. Isosurface value = 0.01 e/Å^3.

On the contrary, the phase pattern of HOMO in ACA is not determined by the position of the vinyl group in the carbonyl side; the main differences between the cis and trans HOMO in ACA is the presence of a nodal plane along the molecule in the trans isomer.

The last types of amides considered in this study are the cyclic ones such as VYP and VYPP. The calculated energy differences between the conformers and the dipole moments are reported in Tables 1 and 2, and the potential energy scans for the C(O)−N−C−C dihedral angle are in Figure 8a. The trans isomers are predicted as the lowest-energy ones for both amides at both theoretical levels, with the energy difference increasing with the ring size. Although the energy difference between both isomers is greater for VYPP, the torsional barrier is higher for VYP (∼1 kcal mol^{-1}) with the maximum slightly skewed for VYPP ($\phi_{max} \approx 80°$ for VYPP instead of 90° for VYP). The torsional barriers for these conformational transitions are lower than the aforementioned for linear *N*-substituted amides, because they imply a rotation around the N−C bond instead of the C(O)−N bond, which shows partial double character. The length of the C(O)−N bond is greater for any of the studied cyclic amides than for the linear ones (Table 1, Supporting Information), and thus, the double-bond character decreases. The evolution of the dipole moment with the dihedral angle is shown in Figure 8b; it decreases from cis to trans conformation going first through a minimum and then through a maximum at $\phi \approx$ 60 and 120°, respectively. The calculated HOMO orbitals for VYP are reported in Figure 8; the shape, phase, and thus the electron distribution of both isomers are very similar for both cyclic amides. The phase of the HOMO is not determined by the position of the vinyl group, and the interaction between the vinyl group and the oxygen is only slightly more effective for the cis isomer. Thus, the stabilization of the trans isomer may be produced by steric effects appearing in the cis configuration that increase its energy.

Aqueous Solutions. The molecular electronic wave functions and all molecular properties change substantially on going from gas phase to solution especially in a complex solvent as water. Two different approaches are possible, although combinations of both may also be found in the literature, to treat the solvent effect on molecular properties: (i) explicit solvent, in which discrete solvent molecules are considered, and (ii) continuum solvent, in which the solvent molecules are replaced by a continuum medium, characterized by its dielectric constant, that surrounds a cavity containing the solute molecule. The drawbacks of each approach are well-known;[40] the main advantage of continuum models over discrete ones, apart from being computationally less demanding, is that discrete methods, when coupled with procedures for computing free energy changes, such as free energy perturbation theory or thermodynamic integration, most readily yield relative solvation free energies between related molecules or conformations rather than absolute values, and thus, sampling problems frequently make the simulations unreliable or simply impractical. Although some promising approaches have been studied to solve this drawback, such as the use of the linear response theory,[41] free energies of solvation may be obtained in a better and simpler way by continuum models.

The self-consistent-reaction-field (SCRF) is the main method within the continuum approach. According to this methodology, in solution, the charge distribution of the solute induces a polarization in the surrounding solvent characterized as a dielectric; thus, the polarized solvent generates an electric field, called a reaction field; the self-consistent interaction between the solute charge distribution and that reaction field constitutes the electrostatic contribution to the solvation free energy, ΔG^{ELEC}. Hence the total free energy of solvation, ΔG^{SOL}, is

TABLE 3: Calculated Free Energy of Solvation, ΔG^{SOL}/kcal mol^{-1}, for the Cis and Trans Isomers in Water Solution with the PCM Model and the Reported Theoretical Levels

	NMF	NEF	NMA	NEA	ACA	VYF	VYP	VYPP
HF/6-311++g** cis	−12.52	−12.79	−11.70	−11.65	−11.13	−8.96	−10.58	−9.49
B3LYP/6-311++g** cis	−12.11	−12.26	−11.37	−11.46	−10.63	−8.04	−9.93	
HF/6-311++g** trans	−11.81	−11.40	−11.80	−11.31	−11.36	−8.47	−9.52	−8.10
B3LYP/6-311++g** trans	−11.12	−11.37	−11.38	−10.50	−10.91	−7.70	−8.89	−7.40

divided in two contributions:

$$\Delta G^{SOL} = \Delta G^{ELEC} + \Delta G^{NON-ELEC} \quad (1)$$

where the nonelectrostatic term, $\Delta G^{NON-ELEC}$, also called short-range term, includes cavity, dispersion and repulsion contributions:

$$\Delta G^{NON-ELEC} = \Delta G^{CAV} + \Delta G^{DIS} + \Delta G^{REP} \quad (2)$$

The cavity contribution is the work needed to form the solute cavity, the dispersion contribution results from the London attractive forces between the solute and the solvent, and the usually small repulsive term arises form the quantum exchange-repulsive interactions between the solute and the solvent.

Different methods have been proposed within the SCRF approach; the polarizable continuum model (PCM) is among the most frequently used.[23] In this method, the cavity is defined as interlocking van der Waals spheres centered at atomic positions, and the reaction field is modeled with point charges on the surface of the solute cavity. Different versions of the PCM model may be found in the literature.[42] In this work, the united atom for Hartree−Fock (UAHF) method is used to build the cavity. A constant value of 1.2 was used to scale all the radii and 60 tesserae were used to divide the spherical surfaces. The electrostatic contribution to the total free energy of solvation is divided in three terms: (i) interaction between the unpolarized solute and unpolarized solvent, ΔG_{US} , or (ii) polarized solvent, ΔG_{PS}, and (iii) total energy of the polarized solute , ΔG_{SP}. All the properties are calculated referred to the unperturbed gas-phase SCF.

The calculated properties of the different conformers for the studied amides in water solution are reported in Table 3 and Table 2 (Supporting Information), computed with the PCM model at the HF and B3LYP levels with the 6-311++g** basis set. As reported in Table 1, the models predict the trans conformers to be the most stable ones as in gas phase, except for NEF with HF and VYF with B3LYP.

For NMF, the energy difference between both isomers decreases substantially going from gas phase to water solution, and the PCM/B3LYP/6-311++g** model predicts almost identical energy for both conformers, Table 1. This result is in contrast with experimental spectroscopic data that have shown an abundance of about 8% of the cis isomer in water.[43] Theoretical studies with lower basis sets predict a greater energy difference between both isomers,[17,44] so the basis set has a significant effect on the model predictions. Nevertheless, it is well-known that the relative stabilization of the trans isomer with respect to the cis one decreases when the solvent dielectric constant increases.[44] Table 2 illustrates that the calculated dipole moments are increased considerably under the influence of the reaction field, and the cis isomer shows higher dipole moments than those of the trans isomer. The NMF dipole moment is dominated by the contribution of the C−O group,[44] the increase of this contribution in solution is similar for both isomers. In addition, as discussed in a later section in relation to Figure 10, local interactions of NMF with the closest water molecules may produce very stable cis conformations, that when exposed to a continuum solvent, may yield a stable cis conformation in solution, in agreement with the experimental results.

The total solvation free energies are reported in Table 3, and the different electrostatic and nonelectrostatic contributions are reported in Table 2 (Supporting Information). From the results, it is clear that the cis isomer is better water-solvated than the trans one, mainly because of the electrostatic contribution, considering that the nonelectrostatic term is almost identical for both conformers. The torsional profile for NMF is reported in Figure 9; the solvent increases the height of the barrier 2.75 kcal mol^{-1}, and this could explain that although the difference between the energy of both conformers decreases in solution, the increase of the transition state energy difficults the interconversion between both forms.

For NEF, the energy differences between both conformers also decrease compared with gas-phase results; even the HF level predicts that the cis isomer is more stable (Table 1). Similar to NMF, the energy difference between both isomers in water solution is very small and, therefore, is extremely sensitive to the theoretical level and basis set considered in the calculations. The dipole moments and energies of solvation of the cis isomer are also greater but only slightly higher than those for NMF. The nonelectrostatic contributions to the total solvation free energies are almost equal for both conformers with the electrostatic term contributing to the better solvation of the cis conformer, Table 2 (Supporting Information). As a consequence of the ethyl hydrophobic *N*-substituent, all the nonelectrostatic terms in NEF are greater than for NMF, but the increase of the electrostatic contribution allows a slightly better solvation of NEF compared to NMF. The torsional barrier for NEF, Figure 9, is also increased in solution (about 2.31 kcal mol^{-1}), a value slightly smaller than for NMF. Thus, the properties of NMF and NEF in water solution are pretty close, and the solvation of both molecules is very similar, being determined mainly because of the strong electrostatic contribution to the total free energy of solvation.

The case of NMA is very different; all of the calculations show clearly the trans conformer as the most stable one; even the energy differences are greater than for gas phase (Table 1). These findings are consistent with the experimentally determined very low concentration of the cis isomer in water solution (around 1.5%).[43] The predicted dipole moments and free energies of solvation of both conformers are almost the same, at both theoretical levels, Tables 2 and 3, also in agreement with the literature reported results.[43] Thus, the trans preference of NMA is not diminished by exposing the molecules to water solvent, as it happened for NMF or NEF; this is of great importance for the analysis of the properties of the peptide bond in proteins, for which NMA is frequently used as a model, considering the difference between bonds in the interior of the structure or exposed to a surrounding water medium. If the different contributions to the total energy of solvation are analyzed, Table 2 (Supporting Information), it may be deduced that the ΔG_{PS} term decreases from one to other conformer in almost the same quantity than ΔG_{SP} increases, hence keeping the electrostatic contribution for both conformers almost equal. Considering that the nonelectrostatic term does not change from

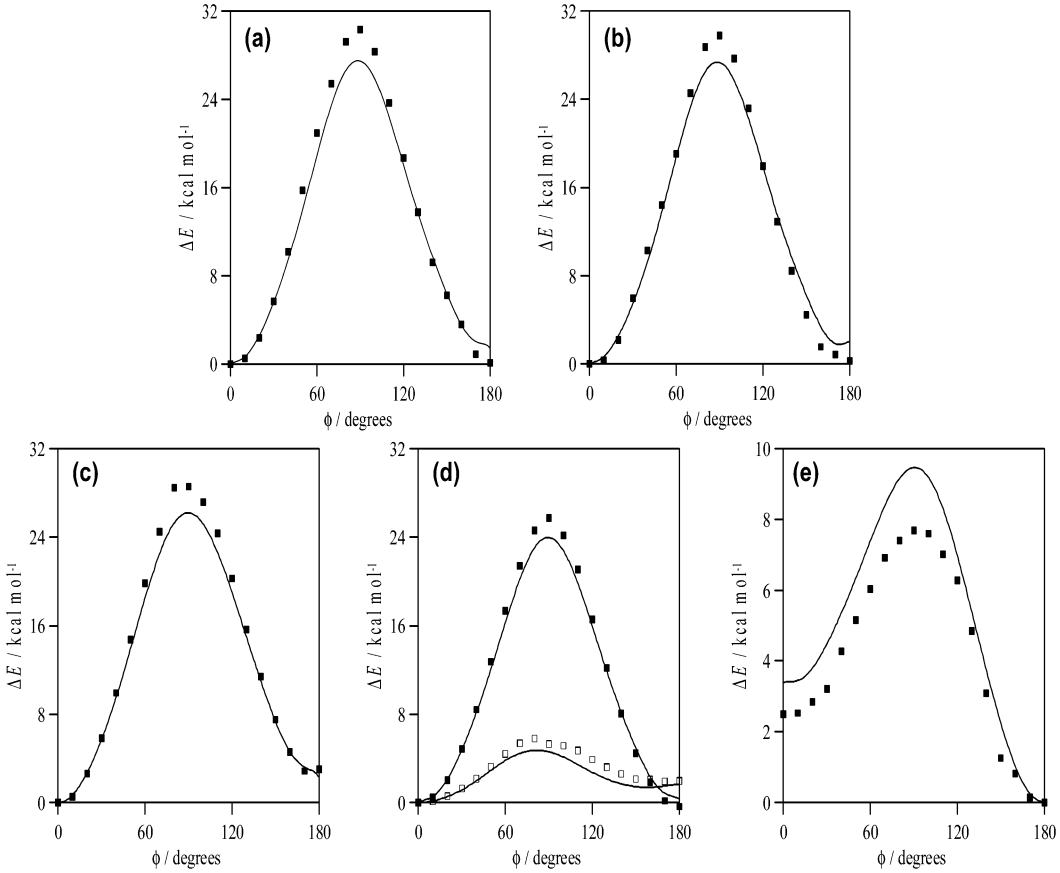

Figure 9. Calculated relaxed potential energy scanning in water solution at PCM/B3LYP/6-31+g* theoretical level. ϕ, dihedral angle; ΔE, energy relatives to the minimum value ($\phi = 0$). (■) water solution, (−) gas phase for comparative purposes. (a) Scanning of the dihedral angle O−C(O)−N−C (3−1−4−6 in Figure 1) of NMF and (b) NEF. (c) Scanning of the dihedral angle O−C(O)−N−C (2−1−3−5 in Figure 1) of NMA. (d) Scanning of the dihedral angle O−C(O)−C−C (3−1−4−6 in Figure 1) of VYF and C(O)−N−C−C (7−6−2−1 in Figure 1) of ACA. (e) Scanning of the dihedral angle C(O)−N−C−C (11−10−13−14 in Figure 1) of VYP.

one to the other conformer, this allows the free energies of solvation of cis and trans NMA to be nearly identical. The calculated torsional barrier for NMA in solution, Figure 9, increases in 2 kcal mol^{-1}, and thus, the configurational ratio is almost unaffected by the surrounding water medium. Hence, the comparison of NMF and NMA results indicates a different effect of the substituents in the carbonyl and nitrogen side of the peptide bond in water medium, in particular on the cis form of NMF, which is more effectively solvated because of its higher dipole moment. When a longer chain is attached to the nitrogen side of the acetamide, NEA, the difference in the properties between both isomers increases, as shown in Tables 1 and 3; although the cis isomer is better solvated, the energy difference with the trans one is lower than in NMA; thus, the presence of the methyl substituent in the carbonyl side of the bond has a strong effect on the molecular properties.

The vinyl group has also very different effects depending on the side of the amide bond in which such group is placed. Results for VYF in water solution, Table 1, shows that the energy differences between both conformers are almost negligible; even the B3LYP theoretical level predicts lower energy for the cis isomer. As in the gas phase, the dipole moment of the trans isomer is greater than that of the cis one with both methods, Table 2, but despite this, the free energy of solvation is greater for the cis isomer, Table 3. The electrostatic and nonelectrostatic contributions to the total free energy of solvation are almost the same for both isomers, Table 2 (Supporting Information). However, when the vinyl group is located in the carbonyl side of the amide bond, ACA, the trans isomer is clearly favored, and the energy differences increase compared to the gas phase for both theoretical levels, Table 1. But as the dipole moments of both conformers of ACA are very similar (Table 2) the free energies of solvation (Table 3) are also close, being only slightly greater for the trans conformer, with no remarkable differences among the different contributions to the total free energies as for VYF, Table 1 (Supporting Information). The torsional profiles calculated for both amides, Figure 9, show the increase of the torsional barriers in water solution.

The conformational behavior of the cyclic amides VYP and VYPP in water solution is also changed going from gas phase to water solution. The energy differences between cis and trans conformers, whose interconversion implies a rotation around the N−C bond, decreases in water, this effect becoming more important as the cycle size increases, as shown in Tables 1 and 3. The reaction field produces a remarkable increase in the dipole moments and increases the differences between the moments of both isomers (Table 2). For these cyclic compounds, the cis isomers are better solvated than the trans ones; this effect is also stronger when the size of the cycle increases, Table 3, but VYP is better solvated than the bigger VYPP molecule. The main differences between the different contributions to the total free energy of solvation among the isomers come from the electrostatic terms, which are remarkably greater for the cis isomer. The effect of the solvent on the torsional profile is reported in Figure 9; in contrast to the other studied amides, for these cyclic molecules, the water solvent decreases the torsional barrier, 1.8 kcal mol^{-1} for VYP, thus making the interconversion between both conformers easier.

Amide Water Complexes. The results of the computations for 1:1 amide−water complexes whose structures were fully

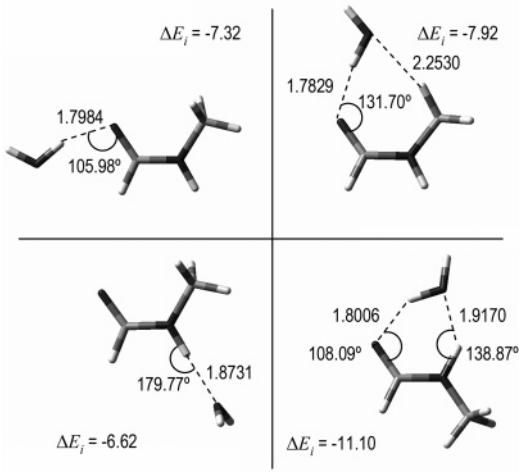

Figure 10. Optimized structures for NMF + water dimers calculated at B3LYP/6-31+g* level, with basis set superposition error removed by the counterpoise procedure. Interatomic distances in Å, angles in deg, and equilibrium binding energies, ΔE_i, in kcal mol^{-1}.

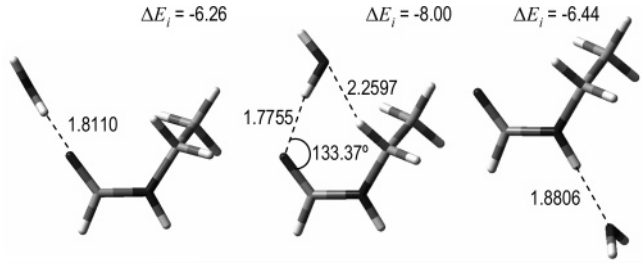

Figure 11. Optimized structures for NEF + water dimers calculated at B3LYP/6-31+g* level, with basis set superposition error removed by the counterpoise procedure. Interatomic distances in Å, angles in deg, and equilibrium binding energies, ΔE_i, in kcal mol^{-1}.

optimized at B3LYP/6-31+g* level are shown in Figures 10−15. The binding energies, ΔE_i, were computed as the difference in total energy between the complex and the sum of isolated, optimized monomers. The main drawback of this kind of computation stands in the basis set superposition error (BSSE), which arises from the fact that the intramolecular description of any of the fragments, monomers, within the complex can be improved with the basis functions of the other fragment, whereas this is not possible in the isolated monomers.[45,46] BSSE produces an artificial overestimation of the binding energies that should be corrected; usually the corrections are done using the so-called counterpoise procedure,[46] which is based on the assumption that if the same basis set is used for the complex and its fragments, monomers, the error is minimized. Although some authors have criticized the method,[47] it is generally accepted that reliable results for intramolecular complexes may be obtained with the counterpoise procedure, and thus, all the binding energies reported in this work have been corrected with it.

Three possible structures of interaction for trans and one for cis conformers of NMF are reported in Figure 10. For the trans isomer, a very stable structure in which the amide acts as proton donor and proton acceptor, with a possible double hydrogen bond between the amide and water molecules, is obtained. The binding energy of this structure is greater than for the first complex reported in Figure 10 in which only a single interaction is established and the amide acts only as a proton acceptor. The interaction through the amide nitrogen proton is also strong, although weaker than the double interaction reported. For the cis isomer, the double interaction through the carbonyl oxygen and nitrogen hydrogen is very strong, giving rise to a very stable structure with the H−O(water) distance in the cis dimer shorter than in the trans conformation. In Figure 11, we report the structures for trans NEF + water dimers, and an NMF structure in which a double bond is formed being more stable than the one with only a single bond through the carbonyl oxygen, with the energy of the double-bonded dimer in NEF being close to the energy for the same complex in NMF. For NEF, the interaction through the amine nitrogen, third one in Figure 11, is also stable. Hence, the presence of a more voluminous group in the nitrogen side of the amide bond decreases the stability of the interaction through the carbonyl oxygen but it does not affect remarkably the interaction through the amine nitrogen.

Three dimer structures for NMA are reported in Figure 12. The interaction through the carbonyl oxygen may be done in two different ways; the second one in Figure 12 is the most stable, although the difference with the first one is small as for

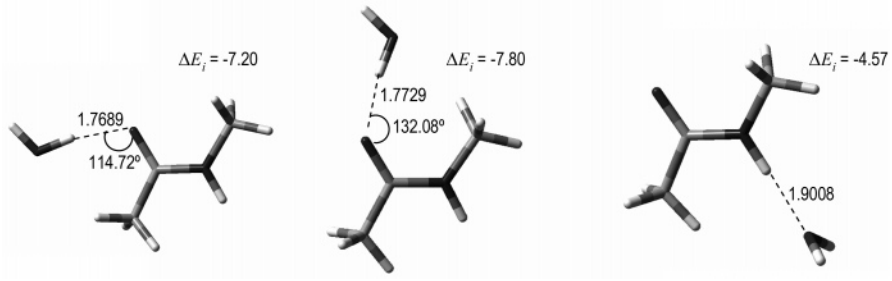

Figure 12. Optimized structures for NMA + water dimers calculated at B3LYP/6-31+g* level, with basis set superposition error removed by the counterpoise procedure. Interatomic distances in Å, angles in deg, and equilibrium binding energies, ΔE_i, in kcal mol^{-1}.

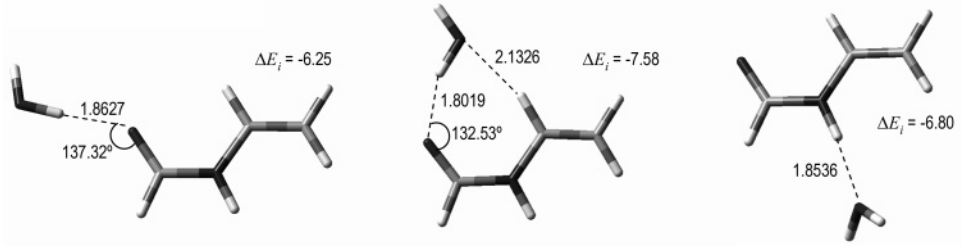

Figure 13. Optimized structures for VYF + water dimers calculated at B3LYP/6-31+g* level, with basis set superposition error removed by the counterpoise procedure. Interatomic distances in Å, angles in deg, and equilibrium binding energies, ΔE_i, in kcal mol^{-1}.

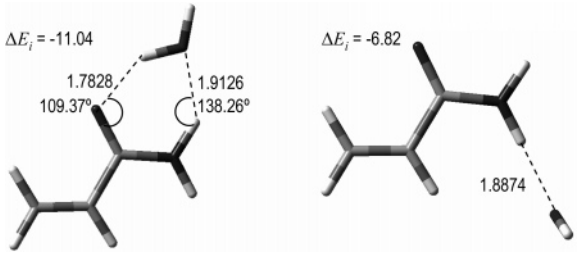

Figure 14. Optimized structures for ACA + water dimers calculated at B3LYP/6-31+g* level, with basis set superposition error removed by the counterpoise procedure. Interatomic distances in Å, angles in deg, and equilibrium binding energies, ΔE_i, in kcal mol^{-1}.

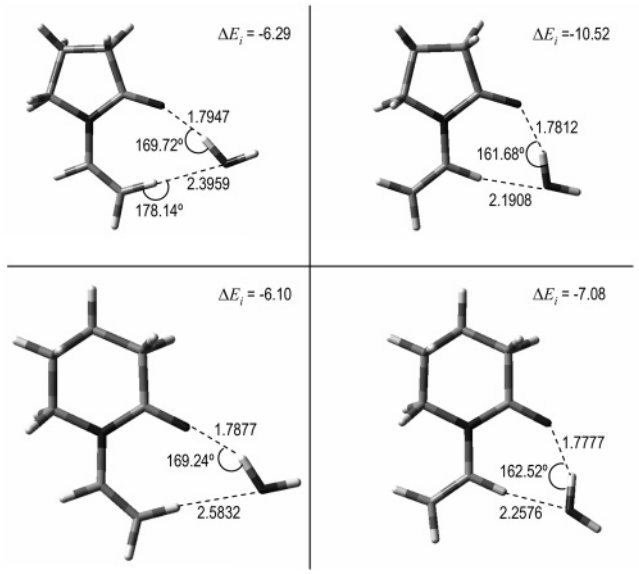

Figure 15. Optimized structures for VYP or VYPP + water dimers calculated at B3LYP/6-31+g* level, with basis set superposition error removed by the counterpoise procedure. Interatomic distances in Å, angles in deg, and equilibrium binding energies, ΔE_i, in kcal mol^{-1}.

NMF. In the second structure, although a double interaction could be proposed, considering that the distance between O(H)−H(CH_3) is 2.4 Å, this second interaction would be weak. The interaction through the amine hydrogen is weaker for NMA than for NMF, although the distance H(N)−O(W) is almost unaffected by the presence of the methyl group in the carbonyl side of the amide bond.

The presence of the vinyl group in the nitrogen side of the amide molecule, VYF, gives rise to strong interactions in the reported complexes, Figure 13. Of the three possible structures, the second one, in which a double hydrogen bond is established, is the most stable one. The planar character of the vinyl group fortifies the second interaction in which the amide acts as a proton donor through the first vinyl hydrogen; the interatomic distance for this interaction, 2.13 Å, is remarkably smaller than the ones reported above for the other amides. Also, the interaction through the amine hydrogen is stronger, and the distance H(N)−O(water) is the shortest among the studied amides. If the vinyl group is in the carbonyl side of the bond, ACA, two main types of interactions may be established, Figure 14. The first structure reported is remarkably stable with a high binding energy because of the simultaneous interaction of the water molecule with the carbonyl oxygen and the aminic hydrogen. The interatomic distances for both hydrogen bonds are very short, and thus, both interactions are strong. The second complex in which the hydrogen bonding is established only through the aminic hydrogen is weaker than the first one.

The complexes formed by cyclic amides are reported in Figure 15. The interaction of the trans isomer with water is stronger than the cis one; a double hydrogen bond is established with short distances in the carbonyl oxygen and vinyl hydrogen interactions; however, in the cis conformers, the interaction through the vinyl hydrogen is weaker, as is shown by the long interatomic distance. As the cycle size increases, the amide−water interaction seems to be reinforced, as is shown by the shorter interatomic distances for both hydrogen bonds in the trans conformation.

Concluding Remarks

The properties and structures of a wide group of selected amides have been studied in the gas phase and a water solution with HF and DFT methods. The trans isomers are the most stable ones for all the studied amides, because of the interaction with the carbonyl oxygen, although the energy differences between both conformations changes substantially going from gas phase to water solution. The torsional energy profiles for the cis/trans configurational transitions show remarkable barrier,s which cause that although the energy differences between the conformers are not too great, the interconversion between them is not favorable, and thus, the trans conformers are the predominant ones. These torsional barriers are increased in water solution except for the cyclic studied amides. The reported study on the properties of the amide/water dimers shows the existence of strong interactions between both molecules that give rise to stable structures with remarkable binding energies.

Acknowledgment. We gratefully acknowledge financial support from Texas A&M University and the USA−Spain Fulbright Commission and Ministerio de Educación y Ciencia (Spain) (SAM).

Supporting Information Available: Calculated parameters of the lowest energy isomers in the gas phase (Table 1), and contributions to the total free energies of solvation according to the PCM model (Table 2). This material is available free of charge via http://pubs.acs.org.

References and Notes

(1) Klotz, I. M.; Franzen, J. S. *J. Am. Chem. Soc*. **1962**, *84*, 3461.
(2) Lawson, E. Q.; Sadler, A. J.; Harmatz, D.; Brandau, D. T.; Micanovic, R.; McElroy, R. D.; Middaugh, C. R. *J. Biol. Chem*. **1984**, *259*, 2910.
(3) Koddermann, T.; Ludwig, R. *Phys. Chem. Chem. Phys.* **2004**, *6*, 1867.
(4) Senes, A.; Ubarretxena, I.; Engelman, D. M. *Proc. Nat. Acad. Sci. U.S.A.* **2001,** *98*, 9056.
(5) Derewenda, Z. S.; Lee, L.; Derewenda, U. *J. Mol. Biol*. **1995**, *252*, 248.
(6) Morozov, A. V.; Kortemme, T.; Tsemekhman, K.; Baker, D. *Proc. Nat. Acad. Sci. U.S.A.* **2004,** 101, 6946.
(7) Langley, C. H.; Allinger, N. L. *J. Phys. Chem. A* **2003**, *107*, 5208.
(8) Vargas, R.; Garza, J.; Dixon, D. A.; Hay, B. P. *J. Am. Chem. Soc*. **2000**, *122*, 4750.
(9) Hammerschmidt, E. G. *Ind. Eng. Chem. Res*. **1934**, *851*, 26.
(10) Carroll, J. *Natural Gas Hydrates: A Guide for Engineers*; Gulf Professional Pub.: Boston, 2003.
(11) Sloan, E. D.; Subramanian, S.; Metthews, P. N.; Lederhos, J. P.; Khokar, A. A. *Ind. Eng. Chem. Res.* **1998**, *37*, 3124.
(12) Storr, M. T.; Rodger, P. M.; Montfort, J. P.; Jussaume, L. A Mechanistic Study of Low Dosage Inhibitors of Clathrate Hydrate Formation. In *Foundations of Molecular Modeling and Simulation*; AIChE Symposium Series No. 325, 2001.
(13) Anderson, B. J.; Tester, J. W.; Borghi, G. P.; Trout, B. L. *J. Am. Chem. Soc*. **2005**, *127*, 17852.
(14) Sloan, E. D. *Clathrate Hydrates of Natural Gases*; Marcel Dekker: New York, 1998.
(15) Carver, T. J.; Drew, M. G. B.; Rodger, P. M. *Phys. Chem. Chem. Phys.* **1999**, *1*, 1807.

(16) Storr, M. T.; Taylor, P. C.; Monfort, J. P.; Rodger, P. M. *J. Am. Chem. Soc*. **2004**, *126*, 1569.
(17) Garcia-Martinez, A.; Teso-Vilar, E.; Garcia-Fraile, A.; Martinez-Ruiz, P. *J. Phys. Chem. A* **2002**, *106*, 4942.
(18) Frisch, M. J.; Trucks, G. W.; Schlegel, H. B.; Scuseria, G. E.; Robb, M. A.; Cheeseman, J. R.; Zakrzewski, V. G.; Montgomery, J. A., Jr.; Stratmann, R. E.; Burant, J. C.; Dapprich, S.; Millam, J. M.; Daniels, A. D.; Kudin, K. N.; Strain, M. C.; Farkas, O.; Tomasi, J.; Barone, V.; Cossi, M.; Cammi, R.; Mennucci, B.; Pomelli, C.; Adamo, C.; Clifford, S.; Ochterski, J.; Petersson, G. A.; Ayala, P. Y.; Cui, Q.; Morokuma, K.; Malick, D. K.; Rabuck, A. D.; Raghavachari, K.; Foresman, J. B.; Cioslowski, J.; Ortiz, J. V.; Stefanov, B. B.; Liu, G.; Liashenko, A.; Piskorz, P.; Komaromi, I.; Gomperts, R.; Martin, R. L.; Fox, D. J.; Keith, T.; Al-Laham, M. A.; Peng, C. Y.; Nanayakkara, A.; Gonzalez, C.; Challacombe, M.; Gill, P. M. W.; Johnson, B. G.; Chen, W.; Wong, M. W.; Andres, J. L.; Head-Gordon, M.; Replogle, E. S.; Pople, J. A. *Gaussian 98*, revision A.11.3; Gaussian, Inc.: Pittsburgh, PA, 2001.
(19) Becke, A. D. *Phys. Rev. A: At., Mol., Opt. Phys.* **1988**, *38*, 3098.
(20) Lee, C.; Yang, W.; Parr. R. G. *Phys. Rev. B: Condens. Matter Mater. Phys.* **1988**, *37*, 785.
(21) Becke, A. D. *J. Chem. Phys.* **1993**, *98*, 5648.
(22) Barone, V. *Chem. Phys. Lett.* **1994**, 226, 392.
(23) Miertus, S.; Scroco, E.; Tomasi, J. *Chem. Phys.* **1981**, *55*, 117.
(24) Cossi, M.; Scalmani, G.; Rega, N.; Barone, V. *J. Chem. Phys.* **2002**, *117*, 43.
(25) Cappelli, C.; Corni, S.; Tomasi, J. *J. Phys. Chem. A* **2001**, *105*, 10807.
(26) Fantoni, A. C.; Caminati, W. *J. Chem. Soc., Faraday Trans*. **1996**, *92*, 346.
(27) Pralat, K.; Jadzyn, J.; Balanicka, S. *J. Phys. Chem*. **1983**, *87*, 1385.
(28) Mantz, Y. A.; Gerard, H.; Iftime, R.; Martyna, G. J. *J. Am. Chem. Soc*. **2004**, *126*, 4080.
(29) Wiberg, K.; Rush, D. J. *J. Org. Chem*. **2002**, *67*, 826.
(30) Lauvergnant, D.; Hiberty, P. C. *J. Am. Chem. Soc*. **1990**, *112*, 6383.
(31) Palmo, K.; Manfors, B.; Mirkin, N. G.; Krimm, S. *Biopolym.* **2003**, *68*, 383.
(32) Fischer, G. *Chem. Soc. Rev.* **2000**, *29*, 119.
(33) Rauk, A.; Glover, S. A. *J. Org. Chem*. **1996**, *61*, 2337.
(34) LaPlanche, L. A.; Rogers, M. T. *J. Am. Chem. Soc.* **1964**, *86*, 337.
(35) Kirsh, Y. E.; Kalninsh, K. K.; Pestov, D. V.; Shatalov, G. V.; Kuznetsov, V. A.; Krylov, A. V. *Russ. J. Phys. Chem.* **1996**, *70*, 802.
(36) Kydd, R. A.; Dunham, R. C. *J. Mol. Struct.* **1980**, *69*, 79.
(37) Marstokk, K. M.; Mollendal, H.; Samdal, S. *J. Mol. Struct.* **2000**, *524*, 69.
(38) Berg, U.; Bladh, N. *J. Comput. Chem*. **1996**, *17*, 396.
(39) Lin, C. K.; Chen, S. Y.; Lien, M. H. *J. Phys. Chem*. **1995**, *99*, 1454.
(40) Duffy, E. M.; Jorgensen, W. L. *J. Am. Chem. Soc.* **2000**, *122*, 2878.
(41) Åqvist, J.; Hansson, T. *J. Phys. Chem*. **1996**, *100*, 9512.
(42) Tomasi, J.; Cammi, R.; Mennucci, B. *Int. J. Quantum Chem*. **1999**, *75*, 783.
(43) Radzicka, A.; Pedersen, L.; Wolfenden, R. *Biochemistry* **1988**, *27*, 4538.
(44) Alagona, G.; Ghio, C.; Igual, J.; Tomasi, J. *J. Mol. Struct.* **1990**, *204*, 253.
(45) Jansen, H. B.; Ross, P. *Chem. Phys. Lett*. **1969**, *3*, 140.
(46) Boys, S. F.; Bernardi, F. *Mol. Phys.* **1970**, *19*, 553.
(47) Frisch, M. J.; DelBene, J. E.; Binkley, J. S.; Schaefer, H. F. *J. Chem. Phys.* **1986**, *84*, 2279.